# InSAR analysis of the San Andreas Fault in Central California

Piyush Agram and Mark Simons
Seismological Laboratory, California Institute of Technology, CA, USA

## Abstract

We present results from Multi-scale InSAR Time Series (MInTS) [1] analysis of L-band (ALOS PALSAR) and C-band (ERS and Envisat) interferometric data sets over Central California. MInTS was designed to exploit the correlation of phase observations over space to improve the signal-to-noise ratio in the estimated deformation time-series compared to the traditional time-series InSAR techniques [2,3]. Traditional time-series analysis techniques assume the statistical independence of InSAR phase measurements over space and time when estimating deformation. However, existing atmospheric phase screen models [4,5] clearly show that noise in InSAR phase observations is correlated over the spatial domain. The MInTS technique reduces the set of InSAR observations to a set of almost uncorrelated coefficients at various spatial scales using wavelets. Traditional inversion techniques can then be applied to the wavelet coefficients more effectively, thus significantly improving the signal-to-noise ratio.

Our results represent the first study of inter-seismic deformation across the Central San Andreas using L-band data. We clearly observe the transfer of offsets from the San Andreas to the Calaveras Fault network just south of Hollister, CA and observe that the offset across the Calaveras Fault persists as far north as San Jose, CA. The region around the Central Calaveras Fault is characterized by heavy decorrelation and previous InSAR studies have failed to reliably estimate the creep rate across this section. The ability of our analysis technique to detect sub cm/yr deformation rates reliably is also demonstrated with example profiles across the Hayward Fault in the Bay Area. We also present evidence for a change in deformation rate in the vicinity of the southern end of the creeping section after the Parkfield, CA possibly driven by a long temporal scale post-seismic mechanism.

## Data and Methodology

**Create Interferograms**
Unwrapped phase
+
Coherence

↓

**Deramping unwrapped IFGs**
Deramp using continuous GPS stations

↓

**Interpolate over holes**
Mask decorrelated areas
+
Interpolate unwrapped phase

↓

**Transform interferograms**
Fast Wavelet Transform (FWT) each unwrapped IFG
+
Compute weights based on coherence mask

↓

**Parameter Estimation**
Estimate temporal parameters for each wavelet coefficient using wavelet weights
+
Covariance model

← **Temporal characterization**
Combination of linear, seasonal and step functions
+
Design matrix of IFG network

↓

**Reconstruction**
Reconstruct each temporal component using IWT
+
Combine for time-series

↓

**Uncertainty Estimates**
Compute uncertainty using a Jackknife procedure

**Figure 1.** Detailed flowchart of the various processing stages in our MInTS analysis of the InSAR data sets [1].

We used all the ALOS PALSAR data (23 cm wavelength) acquired over the San Andreas Fault in the FBD and FBS modes, and available in the ASF archives from Jan 2007 to Dec 2010 for our time-series analysis. All the ALOS PALSAR images were acquired during the ascending passes of the satellite. The Stanford mocomp processor [6] was used to generate the interferometric products and SNAPHU [7] was used to unwrap the interferograms prior to analysis with MInTS.

We also processed Envisat and ERS interferograms covering the area around Parkfield (Track 256, Frame 2889) using ROI-PAC [8]. All processed C-band data was acquired during the descending passes. This C-band (5.6 cm wavelength) dataset spans the time-period from Nov 1992 to Aug 2010 , and includes the 2004 Parkfield earthquake.

In this work, we modeled the line-of-sight (LOS) deformation as a combination of a constant velocity term and a seasonal sinusoidal term for the ALOS PALSAR dataset. The time-series analysis was performed on each frame separately and the final products were combined on a geolocated grid. The detailed description of the MInTS framework is presented as flowchart in Figure 2. In case of the C-band dataset, we included a step function to represent the co-seismic deformation and any rapid deformation that immediately followed the Parkfield EQ.

## L-band analysis

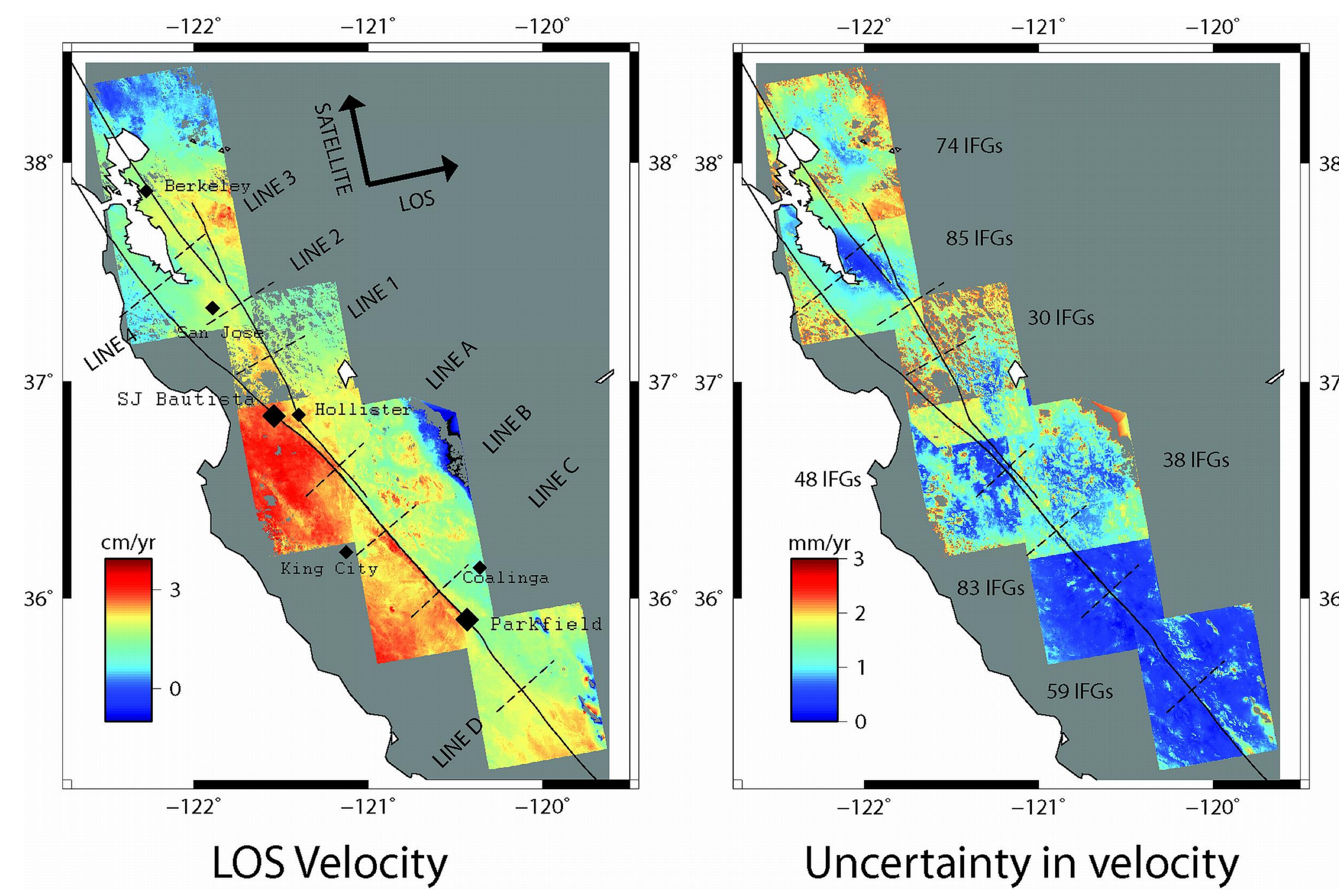


**Figure 2.** LOS velocity (Left) and the associate uncertainty (Right) mosaics of 7 different ALOS PALSAR frames covering Central California. The USGS traces for the San Andreas, Calaveras and Hayward Faults are also shown. 8 dotted line segments represent the location of the velocity profile lines shown in Figures 3 and 4. Number of interferograms used to generate the velocity map is also indicated in the uncertainty plot (Right).

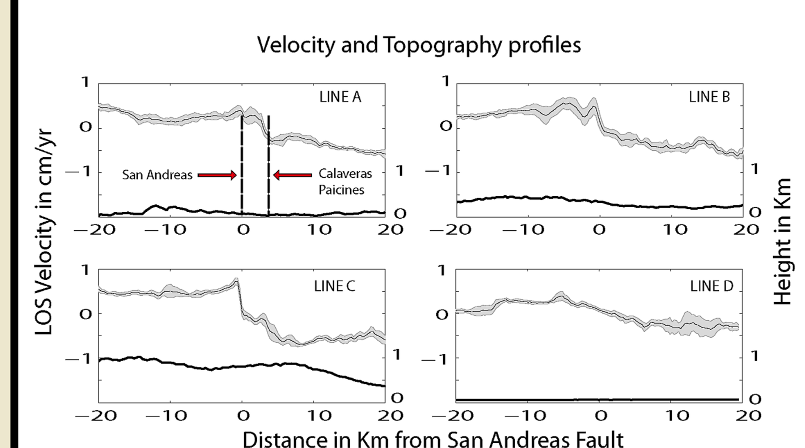


**Figure 3.** LOS velocity profiles (shaded) and topography profiles (solid) plotted along the dotted lines across the San Andreas Fault as shown in Figure 2. A region of 6 km was averaged along the profile lines.

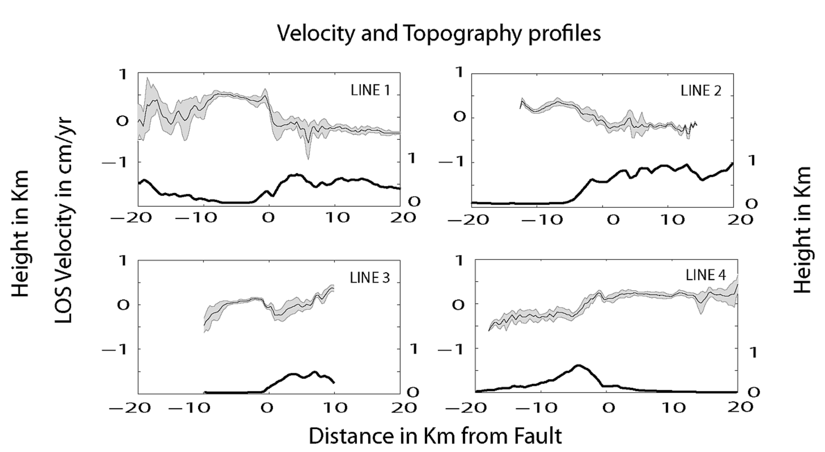


**Figure 4.** LOS velocity profiles (shaded) and topography profiles (solid) plotted along the dotted lines across the Calaveras and Hayward Faults as shown in Figure 2. A region of 6 km was averaged along the profile lines.

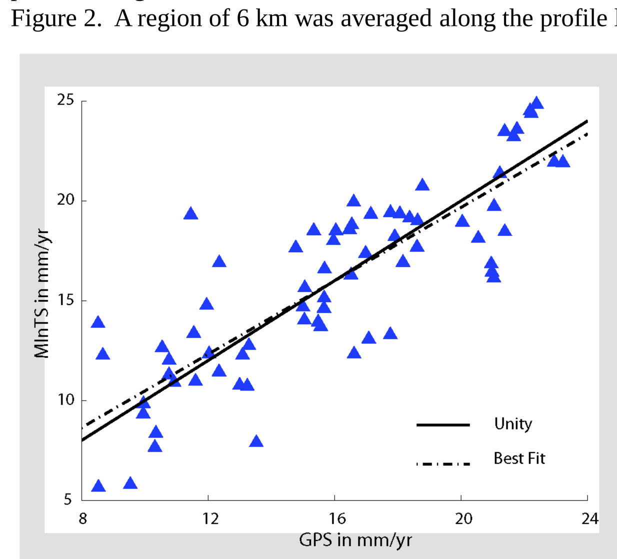


**Figure 5.** Comparison of MInTS LOS velocity estimates with GPS velocities projected into the satellite LOS for 69 PBO stations. The vertical components of the GPS were ignored and only the horizontal components were used for the comparison. Best filt line has a slop of 0.98 and rms value of 2mm.

- The creeping section of the San Andreas Fault is clearly visible in the ALOS stacks (Figure 3). Surface creep across the Hayward and Calaveras Faults are also observed (Figure 4).
- This represents the first InSAR surface observations of creep across the Central Calaveras section (Lines 1 and 2 in Figure 4).
- The discrepancy between InSAR observations and LOS projected GPS velocities is on the order of 2 mm/yr. This is approximately twice that observed at C-band.
- Single LOS observation prevents us from separating horizontal and vertical deformation, particularly close to the fault.

## Estimating Uncertainty

We developed a variant of the statistical Jack-knife procedure to compute uncertainties in the various estimated parameters. Set of InSAR phase observations in a network of interferograms, is correlated due to the inclusion of a single SAR image in many interferograms. Hence, conventional statistical techniques, that assume independent set of observations are no longer applicable. Hence, we determine uncertainties as follows:

1. We create sub-networks from the main interferogram network by removing all interferograms corresponding to individual SAR scene, for each of the SAR scenes.
2. We re-estimate the parameters of interest for each of these sub-networks.
3. We realize that the a single interferogram participates in many of these sub-networks and hence, these sets of estimated parameters are correlated.
4. We compute an approximate correlation matrix, taking into account the number of common interferograms between each of the sub-networks.
5. We reduce the problem to one of determining the mean and variance of a correlated set of observations, using our correlation matrix from Step 4.

All the uncertainties shown in this poster, were derived using the procedure described above.

## C-band analysis

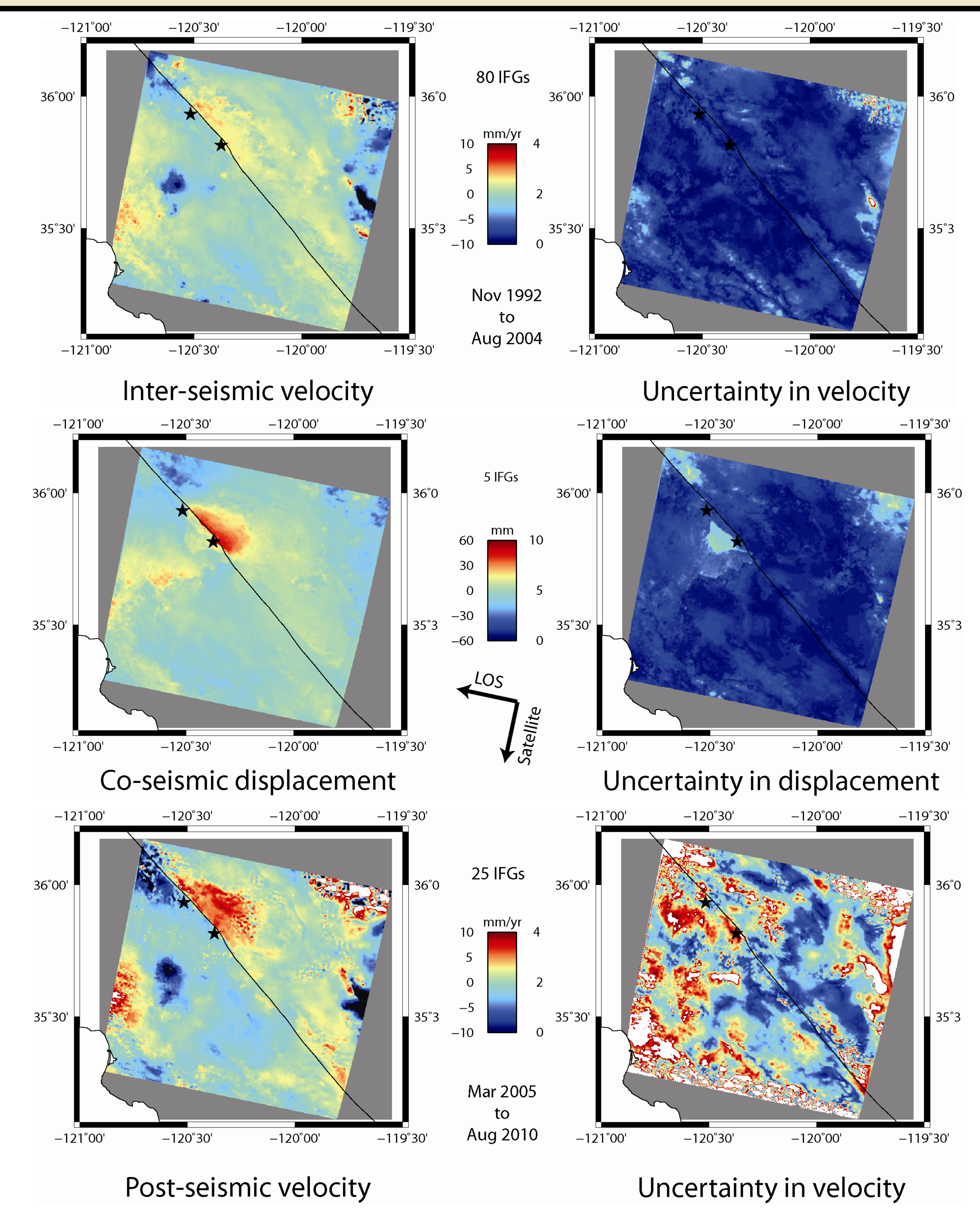


**Figure 6.** Estimated MInTS parameters and associated uncertainties for the C-band stack around Parkfield, CA. The epicenters of the 1966 and 2004 earthquakes are also shown. The number of interferograms and time-span of each of the stacks is also shown. The co-seismic displacements shown includes the rapid deformation (1 month time-scale) following the 2004 earthquake.

- The C-band stacks clearly show the transition zone between the creeping and locked sections of the San Andreas Fault around Parkfield, CA.
- C-band dataset spans a longer time-period (1992-2010) but is less coherent than that L-band stacks generated over the same region.
- L-band interferogram networks are highly redundant, whereas C-band networks are sparse. Most C-band SAR scenes participate in only one or two interferograms.
- The average LOS velocity after the 2004 Parkfield EQ is significantly higher than the inter-seismic rate, possibly due to the effect of long temporal scale post-seismic deformation mechanisms.

## Things To Do

1. Process more C-band stacks acquired on descending passes.
2. Use the L-band and C-band stacks with GPS observations to generate a 3D inter-seismic displacement map for Central California.
3. Include sparse parameter estimation in MInTS for better modeling of EQ time-series.
4. Model the estimated 3D velocities, taking into account the associated uncertainties, using a Bayesian approach.

## References

[1] Hetland, E., Muse, P., Simons, M., Shanker, P., Lin, N., & DiCaprio, C. J. 2011. A multi-scale approach to InSAR time-series analysis. Submitted to JGR – Solid Earth.
[2] Ferretti, A. et al., 2001. Permanent scatterers in sar interferometry. IEEE TGRS 39 (1).
[3] Berardino, P. et al., 2002. A new algorithm for surface deformation monitoring based on small baseline differential sar interferograms. IEEE TGRS 40 (11).
[4] Hanssen, R. F., 2001. Radar Interferometry: Data Interpretation and Error Analysis. 1st ed. Springer.
[5] Emardson, T. R. et al., 2003. Neutral atmospheric delay in interferometric synthetic aperture radar applications: Statistical description and mitigation. JGR 15 (B5), 2231.
[6] Zebker, H. A. et al., 2011. Geodetically accurate InSAR data processor. IEEE TGRS 48(12).
[7] Chen, C. W. et al., 2001. Two-dimensional phase unwrapping with use of statistical models for cost functions in nonlinear optimization. JOSA A 18(2).
[8] Rosen, P., Hensley, S., Peltzer, G., & Simons, M. 2004. Updated repeat orbit interferometry package released. EOS Trans. 85(5).